AIP Journal of Applied Physics

Electric-field induced strain modulation of magnetization in Fe-Ga/Pb(Mg1/3Nb2/3)-PbTiO3 magnetoelectric heterostructures

Yue Zhang, Zhiguang Wang, Yaojin Wang, Chengtao Luo, Jiefang Li, and Dwight Viehland

Citation: Journal of Applied Physics **115**, 084101 (2014); doi: 10.1063/1.4866495
View online: http://dx.doi.org/10.1063/1.4866495
View Table of Contents: http://scitation.aip.org/content/aip/journal/jap/115/8?ver=pdfcov
Published by the AIP Publishing

Electric-field induced strain modulation of magnetization in Fe-Ga/Pb($Mg_{1/3}Nb_{2/3}$)-$PbTiO_3$ magnetoelectric heterostructures

Yue Zhang,[a] Zhiguang Wang, Yaojin Wang, Chengtao Luo, Jiefang Li, and Dwight Viehland
Department of Materials Science and Engineering, Virginia Tech, Blacksburg, Virginia 24061, USA

(Received 9 December 2013; accepted 8 February 2014; published online 24 February 2014)

Magnetostrictive Fe-Ga thin layers were deposited on ⟨110⟩-oriented Pb($Mg_{1/3}Nb_{2/3}$)-30%$PbTiO_3$ (PMN-30%PT) substrates by pulsed laser deposition. The as-prepared heterostructures showed columnar arrays aligned in the out-of-plane direction. Transmission electron microscopy revealed nanocrystalline regions within the columnar arrays of the Fe-Ga film. The heterostructure exhibited a strong converse magnetoelectric coupling effect of up to 4.55×10^{-7} s m^{-1}, as well as an electric field tunability of the in-plane magnetic anisotropy. Furthermore, the remanent magnetization states of the Fe-Ga films can be reversibly and irreversibly changed by external electric fields, suggesting a promising and robust application in magnetic random access memories and spintronics. © *2014 AIP Publishing LLC*. [http://dx.doi.org/10.1063/1.4866495]

INTRODUCTION

Magnetization manipulation in ferromagnets through an electro-mechanical-magnetic coupling mechanism has been reported in multiferroic composites and is known as the converse magnetoelectric effect (CME).[1,2] The most commonly and intensively studied material architectures are two-phase ferromagnetic (FM)/ferroelectric (FE) heterostructures, as they offer fundamental and technological significance.[3–11] In these heterostructures, the coupling between electric and magnetic orderings is achieved by electric field induced strain, through the combination of inverse piezoelectric effect and magnetostriction at the interface. Electric field tunability of magnetization is particularly appealing because of its potential attributes that meet the requirements of high density magnetic data storage at small length scales. Currently, there are several schemes reported that allow for the electric control of magnetization, the most representative examples of which include the spin-torque effect in spin-valves and magnetic tunnel junctions (MTJs),[12] direct interaction between electric field controlled ferroelectric and ferromagnetic polarizations in single phase multiferroics,[13,14] and magnetoelastic interaction between them in multiferroic composites.[15,16] In particular, electric field control of magnetization through elastic interaction opens up an efficient and practical approach to multi-functionalities, such as strain-mediated magnetoelectric random access memory[17] with ultra-high storage density. Since the first development by researchers at the magnetic materials group at the Naval Surface Warfare Center (NSWC), Fe-Ga alloys have been a topic of consistent research interests due to a combination of its relatively large magnetostriction, low saturation fields, high mechanical strength, good ductility, and low cost.[18–23]

In this study, Fe-19%Ga/PMN-30%PT heterostructures were fabricated and their magnetoelectric coupling and the electric field tunability of magnetization via induced strain were investigated. To achieve significant coupling and efficient transfer of strain in these heterostructures, it is essential to choose a ferromagnetic phase with high magnetostriction and a ferroelectric substrate with high piezoelectricity.[8] It has been reported that Fe-19%Ga alloys (i.e., galfenol) have a high magnetostriction of ∼350 ppm at low coercive fields of ∼100 Oe near room temperature.[24] The maximum magnetostriction in Fe-Ga alloys occurs for x ≈ 19 at. % when a mixed phase region of disordered body-centered-cubic α-Fe (A2) and $D0_3$ (ordered bcc) structures co-exists, which has been analogized to electrostriction of ferroelectrics near their morphotropic phase boundaries (MPB).[25,26] Ultrahigh transverse piezoelectric coefficients of $d_{31} \sim -3100$ pC/N and high transverse strain of up to 0.33% have been reported for ⟨110⟩-oriented PMN-29.5%PT single crystal substrates,[27] which far exceeds the value of the ⟨001⟩ and ⟨111⟩ orientations. The high transverse strain is a result of an electric field induced rhombhedral (R) to orthorhombic (O) phase transition. In the present investigation, this tunable strain of PMN-PT was utilized to modulate the magnetization of Fe-Ga films. Furthermore, the in-plane piezoelectric coefficients d_{31} and d_{32} have different signs, consequently the anisotropy of the transverse strains ε_1 and ε_2 in ⟨110⟩ PMN-PT single crystal substrates could significantly contribute to large changes in the in-plane magnetic anisotropy of Fe-Ga films under external applied electric fields, as will be discussed in detail below.

EXPERIMENTS

Films of Fe-Ga with a 50 nm thickness were deposited on ⟨110⟩-oriented PMN-30%PT substrates with dimensions of 4 mm × 5.9 mm × 0.33 mm by pulsed laser deposition (PLD) in an Ar atmosphere at room temperature. The base pressure was 2.5×10^{-5} Torr and the deposition pressure 4 mTorr. The crystal structures of the as-deposited Fe-Ga/PMN-PT heterostructures were characterized by a PANalytical X-ray diffractometer in 2θ-ω scan, and the morphology features were studied by transmission electron microscopy (JEOL 2100). Investigations of electric field manipulation of the magnetization for the Fe-Ga films were performed using a vibrating sample magnetometer (VSM, Lakeshore 7300) at room temperature.

[a]E-mail: yuezhang@vt.edu

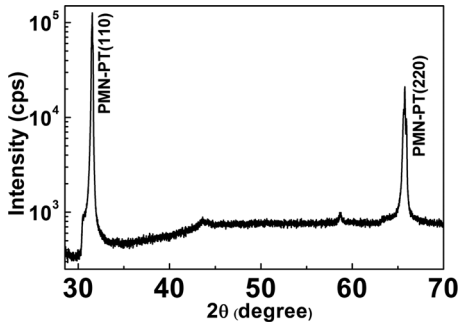

FIG. 1. XRD 2θ-ω line scan of Fe-Ga/PMN-PT heterostructure.

RESULTS AND DISCUSSIONS

Figure 1 shows a XRD 2θ-ω line scan of a Fe-Ga/PMN-PT heterostructure with obvious $\langle 110 \rangle$ peaks of the PMN-PT substrates. However, no apparent diffraction peak from the Fe-Ga film could be detected in the pattern. This indicates that the Fe-Ga film did not epitaxially grow on the PMN-PT substrate owing to the large lattice mismatch.

To better understand the structure of the as-prepared Fe-Ga/PMN-PT heterostructure, a TEM was used to obtain bright field images and selected area electron diffraction (SAED) patterns, as summarized in Figure 2. The bright field image in part (a) demonstrates that the as-deposited Fe-Ga films have a highly organized columnar-like morphology with a diameter of ~5 nm. A higher magnification image in part (b) shows that the columns consist of many separate nanocrystals. By comparison, from the SAED patterns taken from regions of the ion-milled sample for both the Fe-Ga/PMN-PT heterostructure (Fig. 2(c)) and Fe-Ga film (Fig. 2(d)) alone, one can notice that the lattice of the PMN-PT substrates gives strong peaks in the pattern whereas the Fe-Ga film yields only weak diffraction rings. These data clearly demonstrate that the Fe-Ga film on the heterostructures has short-range nanocrystalline ordering in its microstructure. The [111] diffraction rings of the Fe-Ga film coincided with the [200] diffraction peak of the PMN-PT substrate, allowing for coherent growth and interface matching. It is important to note that the lack of long-range crystalline order in the Fe-Ga film may be essential in promoting the overall contribution of the magnetoelastic anisotropy to the total magnetic free energy over that of the magnetocrystalline anisotropy, as the latter in this case should be negligible. In turn, this should enable large changes in the free energy by imposed elastic strain fields.

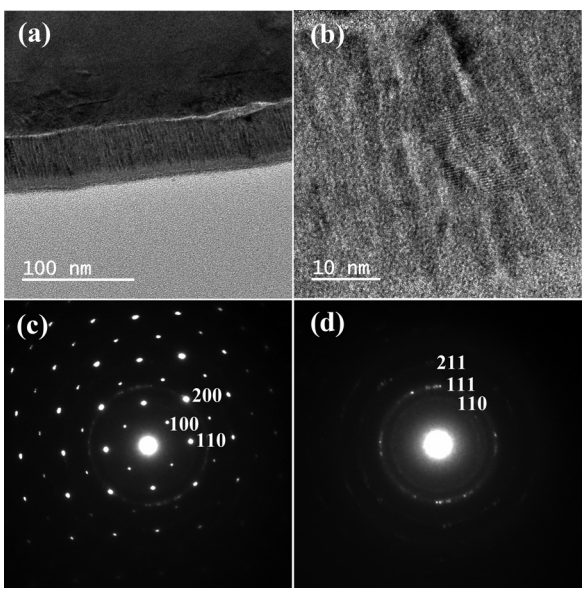

FIG. 2. Transmission electron microscopy (TEM) images of the Fe-Ga/PMN-30PT heterostructure. (a) and (b) bright field images with scale bars of 100 nm and 10 nm, respectively; (c) SAED pattern for both Fe-Ga film and PMN-PT substrate; (d) SAED pattern for Fe-Ga film alone.

Next, changes in the magnetic responses of the as-deposited Fe-Ga film induced by an external applied electric field were investigated *in-situ* using a VSM. A DC electric field was applied along the [110] out-of-plane direction and the corresponding magnetic changes in the Fe-Ga film were measured using VSM. A schematic illustration of the crystallographic geometry of the heterostructure is given in Figure 3(b). The orientation of the external magnetic field $\boldsymbol{H}$ and magnetization $\boldsymbol{M}$ is annotated in the diagram.

The magnetic hysteresis loops in Figure 3(a) provide a clear demonstration of the large shape anisotropy in the vertical direction versus the film plane. These measurements were obtained under zero electric field. The in-plane directions exhibited M-H hysteresis behaviors typical of that previously reported for bulk Fe-Ga alloys.[18–23] However, the column arrays that stand in the out-of-plane direction resulted in this orientation being magnetically harder.

The M-H loops in the in-plane [001], [1$\bar{1}$0] and out-of-plane [110] directions were then measured as a function of electric field, as shown in Figures 3(c) and 3(d). These M-H loops can be seen to exhibit considerable changes with $\boldsymbol{E}$ in both the remanence and coercivity along the in-plane [001] and [1$\bar{1}$0] directions, but hardly any changes could be observed in the out-of-plane direction. With increasing $\boldsymbol{E}$, the remanent magnetization (M_r) of the Fe-Ga film in the [001] in-plane direction decreased notably while its coercive field increased significantly, as can be seen in Figs. 3(e) and 3(f). On the contrary, along the [1$\bar{1}$0] in-plane direction, M_r was greatly enhanced with increasing $\boldsymbol{E}$, while H_c was reduced. The change in H_c reached up to 29.5% along [001]ip, which is notably larger than that previously reported in Ni/$BaTiO_3$(10%)[28] and Fe/$BaTiO_3$ samples (20%).[10]

Along the in-plane [001] direction, a maximum plateau in the magnetization squareness and coercive field were found under electric fields of $8 \leq \boldsymbol{E} \leq 12$ kV/cm. Interestingly, this corresponds to a significantly enhanced piezoelectric response of the PMN-30%PT substrate along [001], with a large transverse piezoelectric coefficient d_{31}. In the field range of $8 \leq \boldsymbol{E} \leq 12$ kV/cm, a maximum in the piezoelectric coefficient occurs in PMN-30%PT due to a field induced R→O phase transition. At lower $\boldsymbol{E}$, the strain varies linearly with electric field, and at higher fields, the strain state is constant. It is also interesting to notice that the change in magnetization of the Fe-Ga film, particularly those in M_r/M_s and H_c, is reversible, exhibiting only small hysteresis effects (Figures 3(e) and 3(f)) transferred from those of the ε-E response of the PMN-PT substrate.[27]

To further explore the electric field tunability of the magnetization of Fe-Ga films, the evolution of magnetization

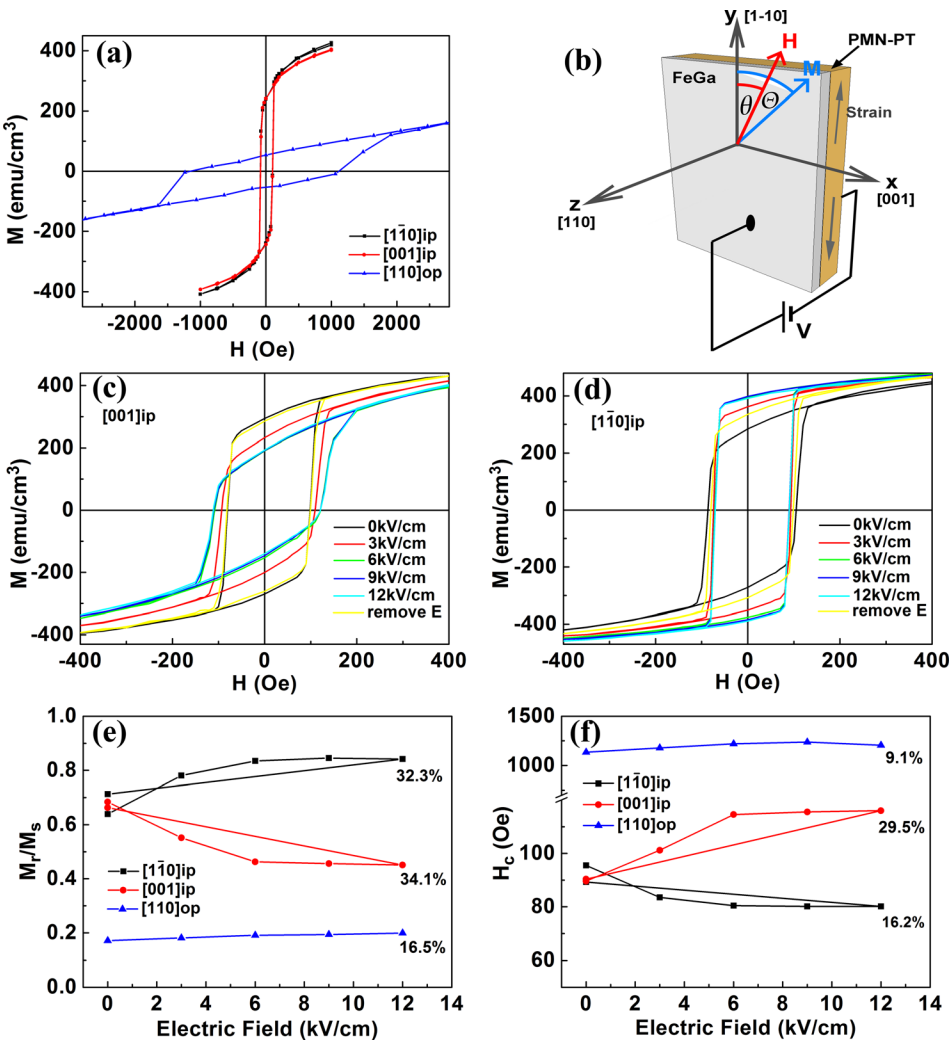

FIG. 3. (a) Comparison of magnetic hysteresis loops obtained from [1$\bar{1}$0] in-plane, [001] in-plane, and [110] out-of-plane direction, respectively. (b) Schematic illustration of the Fe-Ga/PMN-PT heterostructure geometry and the measurement setup. (c) Magnetic hysteresis loops of Fe-Ga/PMN-PT with external magnetic field aligned along in-plane [001] direction. (d) Magnetic hysteresis loops of Fe-Ga/PMN-PT with external magnetic field aligned along in-plane [1$\bar{1}$0] direction. (e) Squareness ratio (M_r/M_s) changes of Fe-Ga/PMN-PT with external electric field. (f) Coercive field changes of Fe-Ga/PMN-PT with external electric field.

$\boldsymbol{M}$ was measured as a function of $\boldsymbol{E}$ and normalized to its poled value $\boldsymbol{M_{pol}}$ at an applied poling electric field of 10 kV/cm. The ferroelectric PMN-PT substrate was poled at 10 kV/cm before the measurements, and the magnetic field $\boldsymbol{H}$ applied along the [001]ip direction was kept constant during each measurement. When the electric field was reduced from 10 kV/cm to −1.8 kV/cm, the Fe-Ga film experiences a decreasing compressive strain due to inverse piezoelectric effects. This leads to a large change of in-plane magnetic anisotropy, which alters the projection of $\boldsymbol{M}$ onto the direction of the external magnetic field. This change reaches its saturation at −1.8 kV/cm. Upon further decrease of $\boldsymbol{E}$ to −10 kV/cm, the value of $\boldsymbol{M}$ returned to its value at E = 10 kV/cm. Please note that the M-E curve exhibits a butterfly shape, rather than being bipolar. This demonstrates that an elastic strain transferred coupling mechanism between the substrate and the film is responsible for the changes in $\boldsymbol{M}$. The maximum magnetization change with $\boldsymbol{E}$ can be seen in Figure 4(b) to reach up to 46% for $\boldsymbol{H} = 0$ Oe. These data demonstrate a highly efficient and deterministic E-control magnetization process. A dramatic decrease of $\boldsymbol{E}$ induced magnetization changes was found with increasing $\boldsymbol{H}$, which is due to the Fe-Ga film being saturated for $\boldsymbol{H} > 500$ Oe.

Figure 4(c) shows the converse magnetoelectric coefficient, which was calculated from the M-E curve for $\boldsymbol{H} = 0$ Oe (Fig. 5(a)) by $\alpha = \mu_0 \Delta M/\Delta E$. The maximum value of the as-derived converse magnetoelectric coefficient was $\alpha = 4.55 \times 10^{-7}$ s m^{-1} for E = −2.7 kV/cm, which field is close to the polarization coercivity of the ferroelectric PMN-PT substrate.[29] The converse ME coefficient is well comparable with the reported value of multiferroic $La_{0.67}Sr_{0.33}MnO_3/BaTiO_3$ heterostructures and other magnetostrictive/piezoelectric laminates.[30]

Next, measurements were performed to determine the $\boldsymbol{E}$ field control of the $\boldsymbol{M}$ orientation. Before each experiment, the sample was poled under $\boldsymbol{H} = -5000$ Oe and $\boldsymbol{E} = 12$ kV/cm, which prepared $\boldsymbol{M}$ into a single domain state. Since $\boldsymbol{H}$ was applied along the in-plane [001] direction ($\theta = 90°$), the measured value of $\boldsymbol{M}$ was the projection of its value onto the [001] direction ($\Theta = 90°$). Measurements were performed under $\boldsymbol{E} = 12$ kV/cm, while $\boldsymbol{H}$ was increased from −5000 Oe to 100 Oe, which is close to but still below the coercive field of the M-H loop. During the $\boldsymbol{H}$ sweep, $\boldsymbol{M}$ remained in its initial orientation for most of the $\boldsymbol{H}$ field range, and only began rotating when $\boldsymbol{H}$ came near 0 Oe (Fig. 5(a)). As $\boldsymbol{H}$ approached the maximum value applied in Fe-Ga (100 Oe), $\boldsymbol{M}$ had not been fully switched. Note at the starting point B_1 of Figure 5(b) that $\boldsymbol{M}$ remains negative while the magnetic field $\boldsymbol{H}$ is positive, indicating that $\boldsymbol{M}$ and $\boldsymbol{H}$ are antiparallel at this point. To demonstrate that $\boldsymbol{M}$ can be

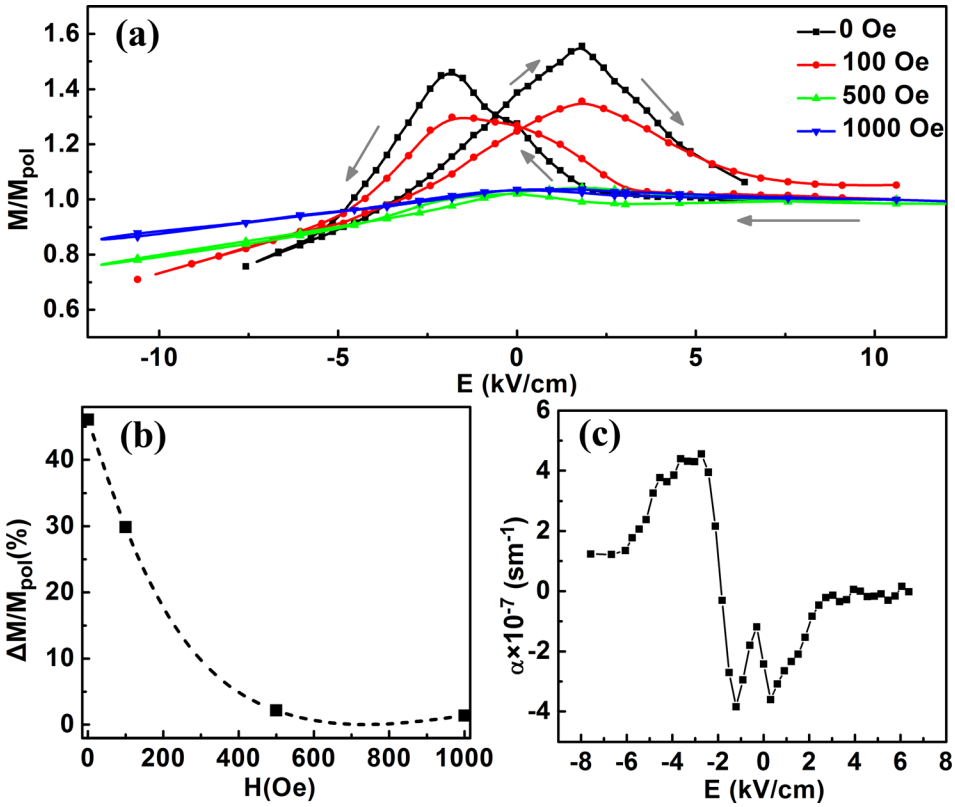

FIG. 4. (a) Magnetization $\boldsymbol{M}$ of Fe-Ga with respect to different electric field $\boldsymbol{E}$ applied across PMN-PT substrate ($\boldsymbol{M}$ is normalized to the value $\boldsymbol{M}_{pol}$ at E = 10 kV/cm). (b) Maximum magnetization change with $\boldsymbol{E}$ as a dependent of $\boldsymbol{H}$. (c) Magnetoelectric coupling coefficient obtained directly from (a) when $\boldsymbol{H} = 0$ Oe.

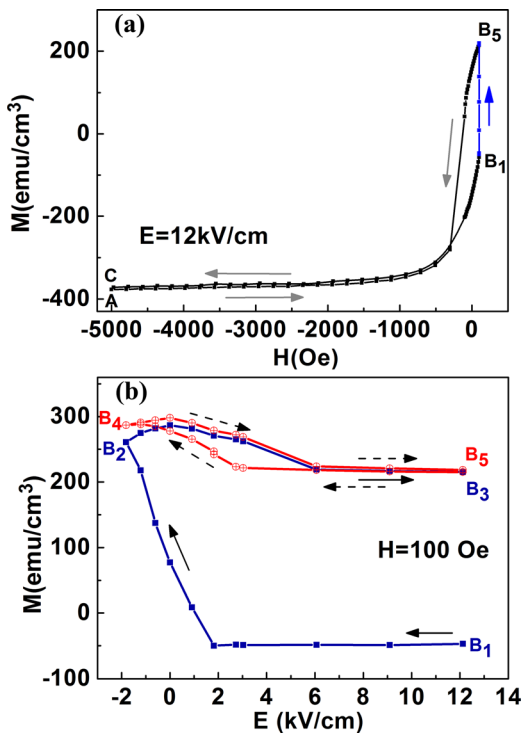

FIG. 5. (a) The magnetization state of Fe-Ga/PMN-PT was prepared by settling electric field to 12 kV/cm and magnetic field to −5000 Oe (at point A); then the magnetic field $\boldsymbol{H}$ was increased from −5000 Oe to 100 Oe when $\boldsymbol{E}$ was kept constant at 12 kV/cm (at point B_1); (b) magnetization manipulation by sweeping the electric field at constant $\boldsymbol{H}$. By sweeping $\boldsymbol{E}$ at $\boldsymbol{H} = 100$ Oe from + 12 kV/cm (B_1) → −1.8 kV/cm (B_2) → +12 kV/cm (B_3), the magnetization $\boldsymbol{M}$ was irreversibly changed (blue line). A second $\boldsymbol{E}$ cycle +12 kV/cm (B_3) → −1.8 kV/cm (B_4) → +12 kV/cm (B_5) only changed $\boldsymbol{M}$ reversibly (red line).

switched solely by changing $\boldsymbol{E}$, the following $\boldsymbol{E}$ sweep was done under constant magnetic field $\boldsymbol{H} = 100$ Oe: + 12 (B_1) → −1.8 (B_2) → + 12 (B_3) kV/cm, and a following sequence of +12 (B_3) → −1.8 (B_4) → +12 (B_5) kV/cm.

Upon decreasing $\boldsymbol{E}$ from 12 kV/cm (B_1) to −1.8 kV/cm (B_2), the orientation of $\boldsymbol{M}$ was completely switched, reaching a nearly demagnetized state ($\boldsymbol{M} = 8.5879$ emu/cc) under $\boldsymbol{E} = 0.9$ kV/cm, and changed sign with decreasing $\boldsymbol{E}$ to be parallel to that of the applied $\boldsymbol{H} = 100$ Oe. On subsequent sweeping of $\boldsymbol{E}$ from −1.8 kV/cm (B_2) back to 12 kV/cm (B_3), $\boldsymbol{M}$ remained positive, and parallel to $\boldsymbol{H}$. A second scan of $\boldsymbol{E}$ from 12 kV/cm (B_3) to −1.8 kV/cm (B_4) and back (B_5) revealed a reversible change in $\boldsymbol{M}$ of only 38.6%, but no switch in its orientation. The small hysteresis in the second cycle corresponds to that in the $\boldsymbol{\varepsilon}$-$\boldsymbol{E}$ loop of ferroelectric substrate. Clearly, a different evolution route of $\boldsymbol{M}$ was observed between these two $\boldsymbol{E}$ sweeps, from 12 to −1.8 kV/cm, where an irreversible $\boldsymbol{M}$ rotation occurred in the first cycle but a reversible one in the second. This demonstrates by sweeping only $\boldsymbol{E}$ that $\boldsymbol{M}$ can be irreversibly switched. To restore the initial state of $\boldsymbol{M}$, $\boldsymbol{H}$ needed to be decreased to the original condition of −5000 Oe (Fig. 5(a)), resulting in resetting the heterostructure back to point C from B_5. This pathway difference in magnetization changes can be understood by its magnetic free energy and that the magnetization must be prepared in a local free energy minimum to allow an irreversible rotation upon changing $\boldsymbol{E}$.[31]

Finally, $\boldsymbol{M}$ was manipulated with periodic electric-field pulses to gain some insights into its reversible responses between two well-defined states. Figure 6 shows that $\boldsymbol{M}$ can be switched between two well-defined electro-remanent states by applying an $\boldsymbol{E}$ field sequence of −0.9 → 0 → 0.9

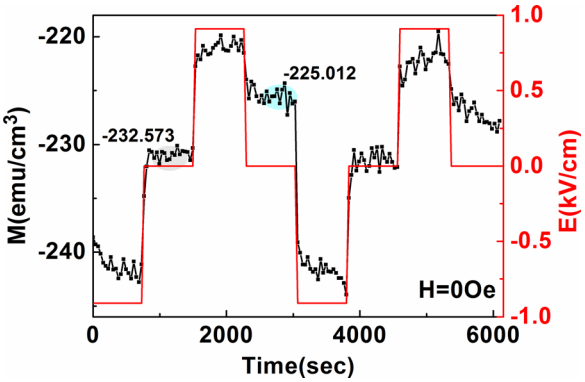

FIG. 6. M sequence with periodically ramping electric field.

$\rightarrow$ 0 kV/cm for $\boldsymbol{H} = 0$ Oe. These data show the ability to reversibly and rapidly tune the magnetization $\boldsymbol{M}$ of Fe-Ga by applying an appropriate electric field. The results demonstrate the potential for application in magnetoelectric read heads in memory devices,[32] and also extend understanding towards modulation of magnetization.

In summary, novel columnar-like Fe-Ga magnetostrictive layers on piezoelectric ⟨110⟩PMN-30%PT substrate have been grown and characterized. These columnar structured Fe-Ga films had droplet-shaped nanocrystalline regions. Films with this morphology exhibited large magnetic shape anisotropy and a large converse magnetoelectric effect. It was shown that an electric field can be utilized to irreversibly and reversibly modulate the magnetization, opening up potential for electric field controlled magnetization devices.

ACKNOWLEDGMENTS

This work was supported by U.S. Department of Energy (DE-FG02-06ER46290).

[1]N. A. Spaldin and M. Fiebig, Science **309**, 391 (2005).
[2]R. Ramesh and N. A. Spaldin, Nature Mater. **6**, 21 (2007).
[3]W. Eerenstein, N. D. Mathur, and J. F. Scott, Nature **442**, 759 (2006).
[4]M. Liu, O. Obi, J. Lou, Y. J. Chen, Z. H. Cai, S. Stoute, M. Espanol, M. Lew, X. Situ, K. S. Ziemer, V. G. Harris, and N. X. Sun, Adv. Funct. Mater. **19**, 1826 (2009)
[5]T. Wu, A. Bur, K. Wong, P. Zhao, C. S. Lynch, P. K. Amiri, K. L. Wang, and G. P. Carman, Appl. Phys. Lett. **98**, 012504 (2011).
[6]G. A. Lebedev, B. Viala, J. Delamare, and O. Cugat, IEEE Trans. Magn. **47**, 4037 (2011).
[7]M. Fiebig, J. Phys. D: Appl. Phys. **38**, R123 (2005).
[8]C. Thiele, K. Doerr, O. Bilani, J. Roedel, and L. Schultz, Phys. Rev. B **75**, 054408 (2007).
[9]F. D. Czeschka, S. Gepraegs, M. Opel, S. T. B. Goennenwein, and R. Gross, Appl. Phys. Lett. **95**, 062508 (2009).
[10]S. Sahoo, S. Polisetty, C.-G. Duan, S. S. Jaswal, E. Y. Tsymbal, and C. Binek, Phys. Rev. B **76**, 092108 (2007).
[11]Z. Wang, Y. Yang, R. Viswan, J. Li, and D. Viehland, Appl. Phys. Lett. **99**, 043110 (2011).
[12]S. Zhang, P. M. Levy, and A. Fert, Phys. Rev. Lett. **88**, 236601 (2002).
[13]T. Lottermoser, T. Lonkai, U. Amann, D. Hohlwein, J. Ihringer, and M. Fiebig, Nature **430**, 541 (2004).
[14]M. Gajek, M. Bibes, S. Fusil, K. Bouzehouane, J. Fontcuberta, A. Barthelemy, and A. Fert, Nature Mater. **6**, 296 (2007).
[15]I. Stolichnov, S. W. E. Riester, H. J. Trodahl, N. Setter, A. W. Rushforth, K. W. Edmonds, R. P. Campion, C. T. Foxon, B. L. Gallagher, and T. Jungwirth, Nature Mater. **7**, 464 (2008).
[16]C. Binek and B. Doudin, J. Phys.: Condens. Matter **17**, L39 (2005).
[17]J. F. Scott, Nature Mater. **6**, 256 (2007).
[18]L. Y. Dai, J. Cullen, M. Wuttig, T. Lograsso, and E. Quandt, J. Appl. Phys. **93**, 8627 (2003).
[19]A. E. Clark, J. B. Restorff, M. Wun-Fogle, T. A. Lograsso, and D. L. Schlagel, IEEE Trans. Magn. **36**, 3238 (2000).
[20]A. E. Clark, K. B. Hathaway, M. Wun-Fogle, J. B. Restorff, T. A. Lograsso, V. M. Keppens, G. Petculescu, and R. A. Taylor, J. Appl. Phys. **93**, 8621 (2003).
[21]N. Srisukhumbowornchai and S. Guruswamy, J. Appl. Phys. **90**, 5680 (2001).
[22]N. Srisukhumbowornchai and S. Guruswamy, J. Appl. Phys. **92**, 5371 (2002).
[23]R. Q. Wu, J. Appl. Phys. **91**, 7358 (2002).
[24]R. A. Kellogg, Ph.D. dissertation, Iowa State University, 2003.
[25]D. Hunter, W. Osborn, K. Wang, N. Kazantseva, J. Hattrick-Simpers, R. Suchoski, R. Takahashi, M. L. Young, A. Mehta, L. A. Bendersky, S. E. Lofland, M. Wuttig, and I. Takeuchi, Nat. Commun. **2**, 518 (2011).
[26]S -E. Park and T. R. Shrout, J. Appl. Phys. **82**, 1804 (1997).
[27]L. H. Luo, H. X. Wang, Y. X. Tang, X. Y. Zhao, Z. Y. Feng, D. Lin, and H. S. Luo, J. Appl. Phys. **99**, 024104 (2006).
[28]S. Gepraegs, A. Brandlmaier, M. Opel, R. Gross, and S. T. B. Goennenwein, Appl. Phys. Lett. **96**, 142509 (2010).
[29]T. Fitchorov, Y. Chen, B. Hu, S. M. Gillette, A. Geiler, C. Vittoria, and V. G. Harris, J. Appl. Phys. **110**, 123916 (2011).
[30]W. Eerenstein, M. Wiora, J. L. Prieto, J. F. Scott, and N. D. Mathur, Nature Mater. **6**, 348 (2007).
[31]M. Weiler, A. Brandlmaier, S. Gepraegs, M. Althammer, M. Opel, C. Bihler, H. Huebl, M. S. Brandt, R. Gross, and S. T. B. Goennenwein, New J. Phys. **11**, 013021 (2009).
[32]Y. Zhang, Z. Li, C. Deng, J. Ma, Y. Lin, and C.-W. Nan, Appl. Phys. Lett. **92**, 152510 (2008).